

Energetics, Charge Transfer and Magnetism of Small Molecules Physisorbed on Phosphorene

Yongqing Cai[†], Qingqing Ke[‡], Gang Zhang^{*†}, and Yong-Wei Zhang^{*†}

[†]Institute of High Performance Computing, A*STAR, Singapore 138632

[‡]Department of Materials Science and Engineering, National University of Singapore, Singapore 117574

ABSTRACT: First-principles calculations are performed to investigate the interaction of physisorbed small molecules, including CO, H₂, H₂O, NH₃, NO, NO₂, and O₂, with phosphorene, and their energetics, charge transfer, and magnetic moment are evaluated on the basis of dispersion corrected density functional theory. Our calculations reveal that CO, H₂, H₂O and NH₃ molecules act as a weak donor, whereas O₂ and NO₂ act as a strong acceptor. While NO molecule donates electrons to graphene, it receives electrons from phosphorene. Among all the investigated molecules, NO₂ has the strongest interaction through hybridizing its frontier orbitals with the 3p orbital of phosphorene. The nontrivial and distinct charge transfer occurring between phosphorene and these physisorbed molecules not only renders phosphorene promising for application as a gas sensor, but also provides an effective route to modulating the polarity and density of carriers in phosphorene. In addition, the binding energy of H₂ on phosphorene is found to be 0.13 eV/H₂, indicating that phosphorene is suitable for both stable room-temperature hydrogen storage and its subsequent facile release.

Supporting Information Placeholder

INTRODUCTION

Recent years have witnessed rapid progress in the synthesis, characterization, and applications of atomically thin two-dimensional (2D) materials, such as graphene and transition metal dichalcogenide (TMD).^{1,2} Graphene has many fascinating properties, based on which, many proof-of-concept devices, such as transistors, supercapacitors and gas sensors, have been demonstrated.³⁻⁶ Nanostructured MoS₂, with a size-independent carrier mobility⁷ and a much smaller thermal conductivity than graphene,^{8,9} has also attracted increasing attention for applications in nanoelectronic and thermoelectric.^{10,11} On the one hand, owing to their ultrathin thickness, high surface-volume ratio and weak electronic screening, properties of monolayer graphene and MoS₂ tend to be strongly affected by physical/chemical adsorbates.¹²⁻¹⁴ On the other hand, a promoted interaction between external molecules and 2D materials not only renders them eligible for sensing applications but also enables the modulation of their electronic and chemical properties.¹⁵⁻¹⁷ For instance, surface modification via hydrogenation was shown to induce a band gap opening in graphene,¹⁸ and ordered hydrogen adsorption on MoS₂ was shown to create a conducting nanoroad.¹⁹

Small molecules, such as CO, H₂, H₂O, NH₃, NO, NO₂, and O₂, are known to be ubiquitously present on 2D materials surfaces, and unsurprisingly, these small molecules can never be fully removed from these surfaces due to their large surface areas.¹¹ Importantly, physisorbed small molecules were found to create marked effects in modifying carriers density, inducing the shift of Fermi level, and modulating the optical properties of graphene and MoS₂.²⁰⁻²⁷ In fact, due to these effects, graphene and MoS₂ were shown to be used as a gas sensor.¹³⁻¹⁶

Recently, phosphorene,²⁸ a new elemental 2D material, has been exfoliated by mechanical cleavage of black phosphorus (BP), the most stable allotrope of the element phosphorus in ambient condition.²⁹ A sizable direct band gap (1.5 eV for monolayer phosphorene) and a large room-temperature mobility up to 1000 cm²V⁻¹s⁻¹ render phosphorene promising for applications in nanoelectronics and optoelectronics.³⁰⁻³² Different from graphene and MoS₂, phosphorene is an intrinsic p-type semiconductor. It is noted that many studies have been devoted to examining various factors on the electronic properties of phosphorene. For example, strong thickness-dependent electronic properties of few-layer phosphorene such as work function, band gap, band alignment have been examined.³³ The effects of layer disorder³⁴ and nanoribbons width,³⁵ and also electronic anisotropy³⁶⁻⁴⁰ of phosphorene have also been analyzed. Despite of these interesting studies, systematic understanding of the effect of physisorbed small molecules, such as CO, H₂, H₂O, NH₃, NO, NO₂, and O₂, on the electronic properties of phosphorene is still lacking. Owing to the marked effects of physisorbed small molecules on graphene and MoS₂, clearly, it is both of scientific interest and technological importance to understand the energetics, charge transfer and magnetism of small molecules physisorbed on phosphorene.

In this work, we perform a systematic theoretical study on the adsorption of small molecules (CO, H₂, H₂O, NH₃, NO, NO₂ and O₂) on phosphorene, focusing on the energetics, magnetic moments, and charge transfer between these molecules and phosphorene. We find that CO, H₂, H₂O, and NH₃ act as charge donors; whereas NO₂, and O₂ serve as charge acceptors. While NO molecule donates electrons to graphene, it accepts electrons from phosphorene. Our present study provides a valuable reference for assessing the effect of physisorbed small molecules on phosphorene. In addition, the present work also demonstrates that the

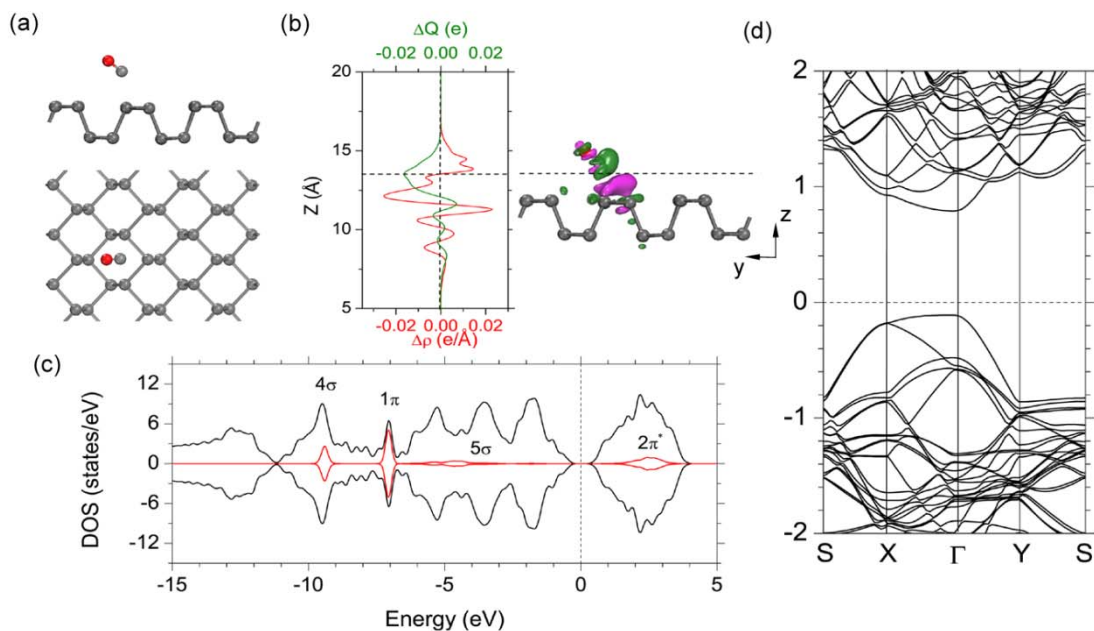


Fig. 1 CO adsorbed on phosphorene. (a) The side and top views of the lowest-energy configuration. The phosphorus, carbon and oxygen atoms are represented by balls in grey, black and red colors, respectively. (b) Plane-averaged differential charge density $\Delta\rho(z)$ (red line), amount of transferred charge $\Delta Q(z)$ (green line), and side view of the 0.005 \AA^{-3} DCD isosurface (right). The violet (green) color denotes diminishing (accumulation) of electrons. (c) DOS of CO on phosphorene (black line), LDOS and positions of the molecular orbitals of CO (red line). (d) Band structure of CO on phosphorene.

electronic properties of phosphorene can be tuned by selective adsorption of those small molecules.

COMPUTATIONAL METHODS

The first-principles calculations are performed within the framework of density functional theory (DFT) by using Vienna ab initio simulation package (VASP) package.⁴¹ Van der Waals (vdW) corrected functional with Becke88 optimization (optB88)⁴² is adopted for analyzing the noncovalent chemical functionalization of phosphorene by small molecules. All the structures are relaxed until the forces exerted on each atom are less than 0.005 eV/\AA . The relaxed lattice constant of monolayer phosphorene is $a=3.335 \text{ \AA}$, $b=4.571 \text{ \AA}$ along zigzag and armchair directions, respectively based on a $14 \times 10 \times 1$ Monkhorst-Pack (MP) grid for k-point sampling. Here we only consider a single molecule adsorption in the $4 \times 3 \times 1$ supercell (48 phosphorus atoms) in the dilute doping limit. The thickness of the vacuum region is greater than 15 \AA . The first Brillouin zone is sampled with a $3 \times 3 \times 1$ MP grid and a kinetic energy cutoff of 400 eV is adopted. The binding energy (E_b) of the molecule to phosphorene is calculated as $E_{\text{Mol+P}} - E_{\text{Mol}} - E_{\text{P}}$, where E_{Mol} , E_{P} and $E_{\text{Mol+P}}$ are the energies of the molecule, phosphorene sheet and molecule adsorbed phosphorene, respectively.

RESULTS

We have examined several possible anchoring positions on the high symmetric sites of all the molecules on the phosphorene surface, including both above the puckered hexagon and the zigzag trough with the molecules being aligned either parallel or

perpendicular to the surface, and the results based on the lowest-energy configurations are compiled in Table 1.

Molecular Donors

In the following, we examine four molecules: CO, H_2 , H_2O , and NH_3 , which have a closed-shell electronic structure and serve as donors.

CO adsorption: For CO adsorption, the most stable binding configuration is shown in Fig. 1a, where the molecule locates above the ridge with the CO bond being aligned perpendicular to the surface with a slight deviation from the normal direction. The C atom has a coordination number of four and forms three weak vdW C-P bonds with the bond length ranges from 3.06 to 3.15 \AA . The vdW-corrected E_b for single CO is -0.31 eV .

To analyze the electronic interaction between the molecule and phosphorene, we calculate the differential charge density (DCD) $\Delta\rho(r)$. The isosurface of the $\Delta\rho(r)$ for the adsorbed CO molecule is depicted in Fig. 1b. It can be seen that there is a large charge redistribution upon CO adsorption, especially between the adsorption gap of the molecules and the P atoms, which significantly disturbs the HOMO state (5σ), which is mainly located on the C atom (see the inset of Fig. 1c). This is also clearly reflected by the local density of states (LDOS) analysis as shown in Fig. 1c, where the CO 5σ state is widely broadened and distributed from -6 to -4 eV below the Fermi level; while the CO $2\pi^*$ (LUMO), 1π (HOMO-1) and 4σ (HOMO-2) states are less affected after the adsorption. For pristine phosphorene, the three peaks below the valence band edge, which are located at around -2 , -3.5 , -5 eV , consist of mainly (p_y, p_z) , (p_x, p_y, p_z) , (p_x, p_y, p_z) hybridizations with a small amount of $3s$ orbital. The broad peaks at -10 eV and -13 eV are mainly comprised of $3s$ state. This indicates that the strong broadening of CO 5σ state mainly arises from the interaction with the phosphorus $3p$ orbitals.

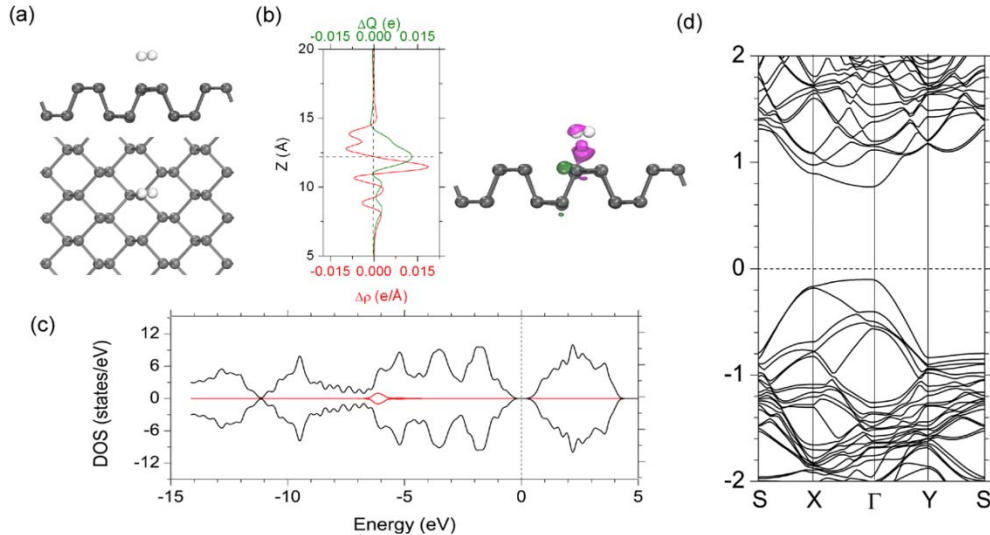


Fig. 2 H_2 adsorbed on phosphorene. (a) The side and top views of the lowest-energy configuration. The phosphorus and hydrogen atoms are represented by balls in grey and white colors, respectively. (b) Plane-averaged differential charge density $\Delta\rho(z)$ (red line), amount of transferred charge $\Delta Q(z)$ (green line), and side view of the 0.005 \AA^{-3} DCD isosurface (right). The violet (green) color denotes diminishing (accumulation) of electrons. (c) DOS of H_2 on phosphorene (black line) and LDOS of H_2 (red line). (d) Band structure of H_2 on phosphorene.

To quantify the amount of charge transfer from the molecule, we calculate the plane-averaged DCD $\Delta\rho(z)$ along the direction normal to the surface by integrating $\Delta\rho(r)$ within the x - y plane. The amount of transferred charge up to z point is obtained using $\Delta Q(z) = \int_{-\infty}^z \Delta\rho(z') dz'$. We plot the $\Delta\rho(z)$ and $\Delta Q(z)$ together with the DCD in Fig. 1b for comparison. The integral of the charge accumulated from the bottom vacuum up to the interface between the adsorbate and the phosphorene (defined as the plane of zero charge variation shown in the $\Delta\rho(z)$ curve) gives the total charge donated by the molecule to the phosphorene. The exact amount of charge transfer normally corresponds to the maximum of the $\Delta Q(z)$ curve at the interface of the adsorbate and the surface.¹⁷ It can be seen that the total charge transfer from the CO to phosphorene amounts to $0.007 e$. Therefore, the CO molecule acts as a weak donor on the phosphorene surface, and the bands of phosphorene (Fig. 1d) are almost unchanged upon CO adsorption. The C-O bond length of the adsorbed CO is 1.15 \AA , which is only slightly increased from that (1.14 \AA) of its gas molecule. Our results are in good agreement with a recent work using local density approximation (LDA) approach in terms of the adsorption configuration and charge transfer between CO and phosphorene.⁴³

H_2 adsorption: The most stable configuration for H_2 adsorption adopts a nearly parallel configuration with the H-H bond being along the armchair direction, and one of the H atom being directly above the P atom with the H-P bond length of 2.46 \AA (Fig. 2a). The E_b is found to be -0.13 eV . The value of E_b is found to be -0.13 eV , which is close to the requirement for an appropriate hydrogen storage with a binding energy of -0.15 – $-0.3 \text{ eV}/H_2$.^{44,45} The intermediate binding energy of hydrogen molecule on phosphorene implies a stable hydrogen storage at ambient conditions and subsequent facile release. It is noted that the E_b of H_2 on phosphorene is much larger than that of H_2 on pristine graphene ($\sim 0.04 \text{ eV}/H_2$),⁴⁶ which suggests a higher working temperature for using phosphorene as the hydrogen adsorbent. However, since the density of bulk phosphorene is about 23% larger than that of graphite, implying a smaller gravimetric value of the hydrogen storage than graphite. Nevertheless, the highly flexible and puckered honeycomb structure of phosphorene implies a higher

possibility for increasing the chemical affinity for hydrogen with convex areas of phosphorene surfaces, which has been demonstrated in fullerenes, nanotubes and graphene by controlling curvature or creating ripples.⁴⁷⁻⁵¹

The isosurface plot of DCD (Fig. 2b) shows that there is a depletion of DCD in H atoms and an accumulation of electrons in the nearest P atom. The hydrogen molecule clearly donates electrons to phosphorene with around $0.013 e$ per molecule. Compared with CO molecule, while the H_2 molecule has a larger amount of charge transfer, its binding energy is smaller. The underlying reason is that the binding mechanism of molecules on surface can be factored into two groups: the covalent interactions accompanying with the charge transfer and electrostatic attractions associated with polarization induced dipole-dipole interaction. For physisorption, the latter can play a more important role. Since the dipole moment of H_2 is zero, the dispersive force and polar-polar interaction between H_2 and phosphorene are much weaker than that of the strongly polarized CO molecule, leading to the lower binding energy despite the fact that the H_2 has a larger charge transfer. The relatively weak interaction is also reflected by the sharp peak in the LDOS of H_2 and the nearly unchanged band structure of adsorbed phosphorene compared with that of the pristine phosphorene, as shown in Fig. 2c and d, respectively.

H_2O adsorption: For the H_2O molecule, we have considered various orientations including the two O-H bonds pointing up or down or parallel to the surface. The most stable configuration is given in Fig. 3a, where one of the O-H bonds is parallel to the surface along the armchair direction and the other nearly normal to the surface. The in-plane O-H bond locates directly above the armchair P-P bond with the O-P bond length of 2.71 \AA , and two H-P bonds of 3.14 and 3.21 \AA . The binding energy is -0.14 eV , almost same as H_2 adsorption. Notably, this configuration is quite similar to the structure of H_2O molecule adsorbed on graphite surface.⁵²

The charge transfer analysis shows that each H_2O donates about $0.035 e$. The relatively large dipole moment of H_2O induces a large charge redistribution even in the opposite side of the adsorbed phosphorene surface.(Fig. 3b) This prominent effect of

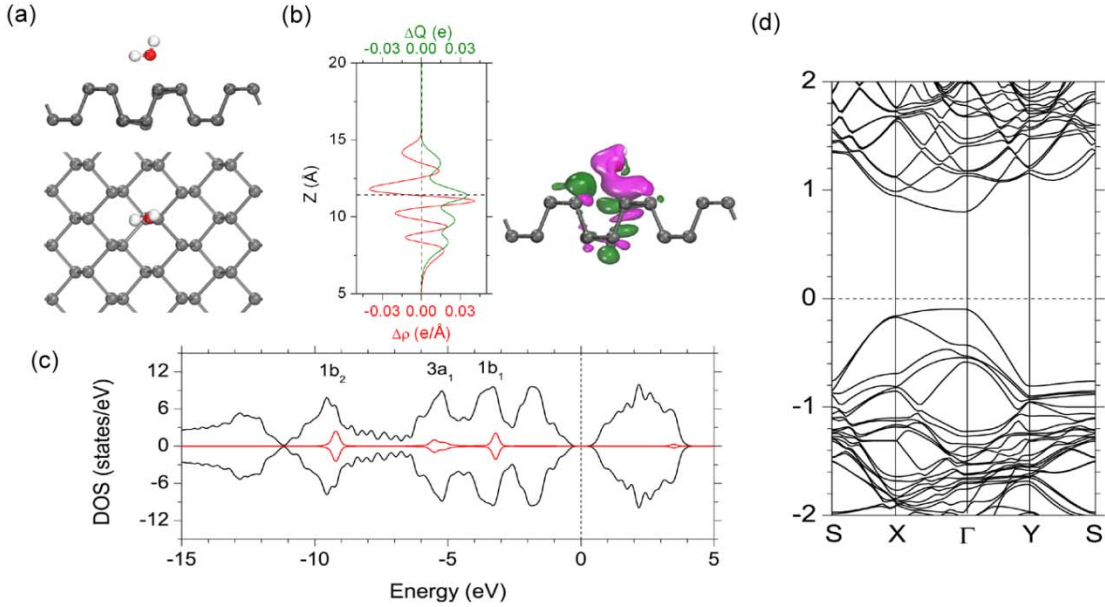


Fig. 3 H₂O adsorbed on phosphorene. (a) The side and top views of the lowest-energy configuration. The phosphorus, oxygen and hydrogen atoms are represented by balls in grey, red and white colors, respectively. (b) Plane-averaged differential charge density $\Delta\rho(z)$ (red line), amount of transferred charge $\Delta Q(z)$ (green line), and side view of the 0.005 \AA^{-3} DCD isosurface (right). The violet (green) color denotes diminishing (accumulation) of electrons. (c) DOS of H₂O on phosphorene (black line) and LDOS and positions of the molecular orbitals of H₂O (red line). (d) Band structure of H₂O on phosphorene.

water on the electronic properties of phosphorene shows that in real device, the water may significantly affect the performance such as durability and carriers mobility. The three highest occupied orbitals of the water molecule are $1b_1$ (HOMO), $3a_1$ (HOMO-1), and $1b_2$ (HOMO-2), which are orthogonal around the oxygen atom. The $3a_1$ state with the orbital nearly being normal to the surface has the largest orbital mixing with the P atom, which allows more efficient charge transfer to the phosphorene layer. This interaction in turn makes the energy level of $3a_1$ state greatly broadened (Fig. 3c) and also a slightly downward shift of this state from the HOMO level compared with the energy diagram of the isolated molecule. Similar to CO and H₂, there is no localized states within the band gap of H₂O decorated phosphorene according to Fig. 3d.

Interestingly, while phosphorene has the same topologically equivalent honeycomb lattice as graphene, the charge state of H₂O is quite different for adsorptions on phosphorene and graphene. Here we show that H₂O acts as a strong donor on monolayer phosphorene surface, in contrast, previous studies show that H₂O is a charge acceptor on graphene surface.¹⁶ This distinctive behavior is attributed to the much larger work function of phosphorene (5.2 eV for monolayer phosphorene), thus more electron transferred from water to phosphorene, compared with that of graphene (4.5 eV). Since the phosphorene layer is an intrinsically *p*-type material with a wealth of holes located at the valence band, the decrease of work function and the upward shift of valence band with increasing the thickness of phosphorene reported recently³³ suggest that the charge transfer from water molecule tends to be highly sensitive to the thickness of phosphorene with less electrons being donated to the multilayer phosphorene compared with the monolayer phosphorene.

NH₃ adsorption: Two different adsorption orientations are considered for NH₃ molecule: the H atoms pointing away from the surface, and the H atoms pointing toward the surface. The strongest binding site is found to be the former with the N atom

located directly above the P atom (Fig. 4a). In this binding scenario, the N-P bond length is 2.59 \AA and the binding energy is -0.18 eV . As depicted in Fig. 4b, the DCD analysis shows that there is a significant charge redistribution between the NH₃ and phosphorene, indicating moderate covalent bonding between NH₃ and phosphorene surface arising mainly from the ionization of the lone electron pair at the N atom in the $3a_1$ (HOMO) state. The NH₃ molecule acts as a donor by transferring around $0.05 e$ to phosphorene. The nonbonding $3a_1$ orbital of NH₃ tends to be more affected by the P atoms as evidenced by the strongly broadened LDOS at the top of the valence band as shown in Fig. 4c. Regarding the band structure, the strong interaction and charge donation alter the top valence band of phosphorene along the Y-S and S-X directions with an upward shift of the band due to the enhanced coulomb interaction.

Molecular Acceptors

We next consider three paramagnetic molecules: NO, NO₂, and O₂, which have an open-shell electronic structure.

NO adsorption: For NO molecule, we consider the same initial adsorption configurations as CO molecule. The lowest energy state (Fig. 5a) is the same as CO molecule, with the N atom having a coordination number of four and forming three N-P bonds with bond length ranging from $2.75\text{-}2.88 \text{ \AA}$, which are smaller than those of CO molecule. The binding energy is found to be -0.32 eV , which is almost the same as that of CO molecule.

The half-filled doubly degenerated NO frontier orbital 2π (HOMO), together with its spin-split partner (LUMO), allows back and forward charge transfer by orbital hybridization with phosphorus orbitals. As shown in Fig. 5b, the plane-averaged DCD shows that there is a charge accumulation in NO molecule whereas a loss of electron of phosphorene. The total amount of transferred charge from phosphorene is $0.074 e$. According to the band structure (Fig. 5d), the singly occupied HOMO state of NO

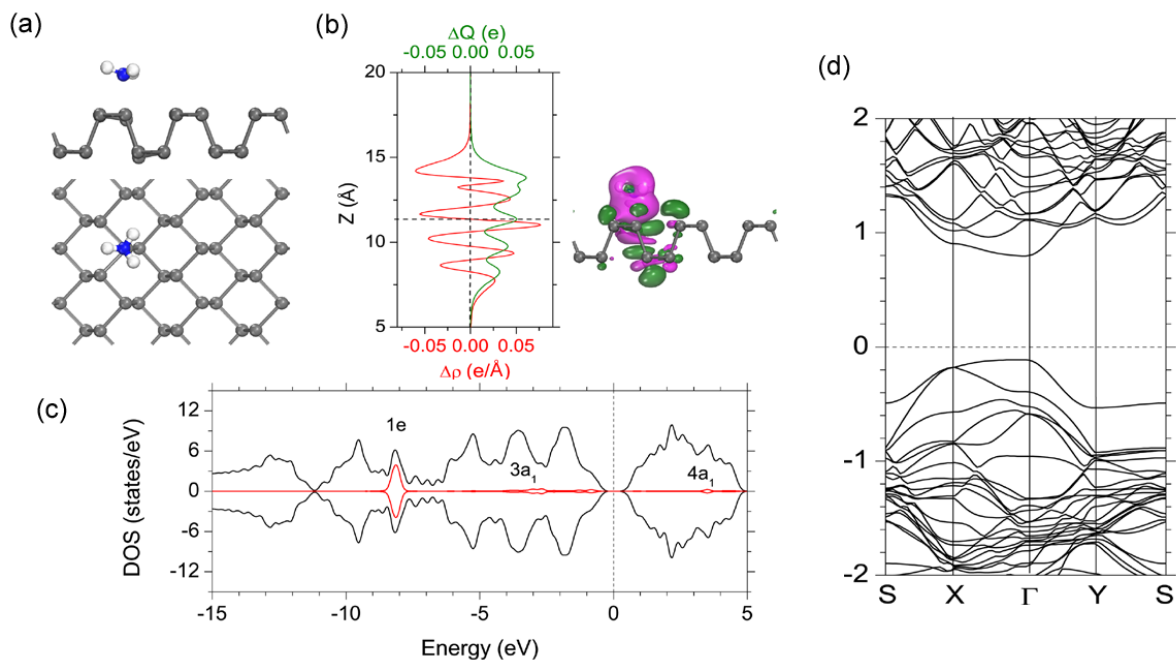


Fig. 4 NH_3 adsorbed on phosphorene. (a) The side and top views of the lowest-energy configuration. The phosphorus, nitrogen and hydrogen atoms are represented by balls in grey, blue and white colors, respectively. (b) Plane-averaged differential charge density $\Delta\rho(z)$ (red line), amount of transferred charge $\Delta Q(z)$ (green line), and side view of the 0.005 \AA^{-3} DCD isosurface (right). The violet (green) color denotes diminishing (accumulation) of electrons. (c) DOS of NH_3 on phosphorene (black line) and LDOS and positions of the molecular orbitals of NH_3 (red line). (d) Band structure of NH_3 on phosphorene.

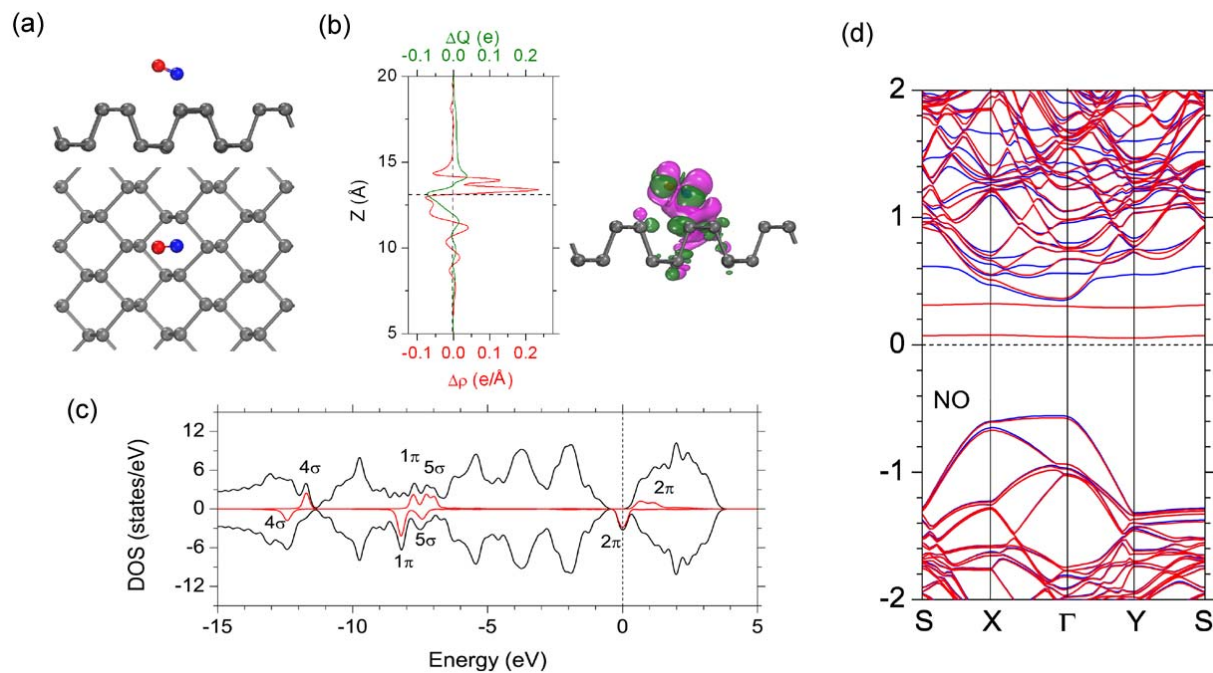


Fig. 5 NO adsorbed on phosphorene. (a) The side and top views of the lowest-energy configuration. The phosphorus, oxygen and nitrogen atoms are represented by balls in grey, red and blue colors, respectively. (b) Plane-averaged differential charge density $\Delta\rho(z)$ (red line), amount of transferred charge $\Delta Q(z)$ (green line), and side view of the 0.005 \AA^{-3} DCD isosurface (right). The violet (green) color denotes diminishing (accumulation) of electrons. (c) DOS of NO on phosphorene (black line) and LDOS and positions of the molecular orbitals of NO (red line). (d) Spin-polarized band structures of NO on phosphorene with spin-up bands and spin-down bands are indicated in blue and red, respectively.

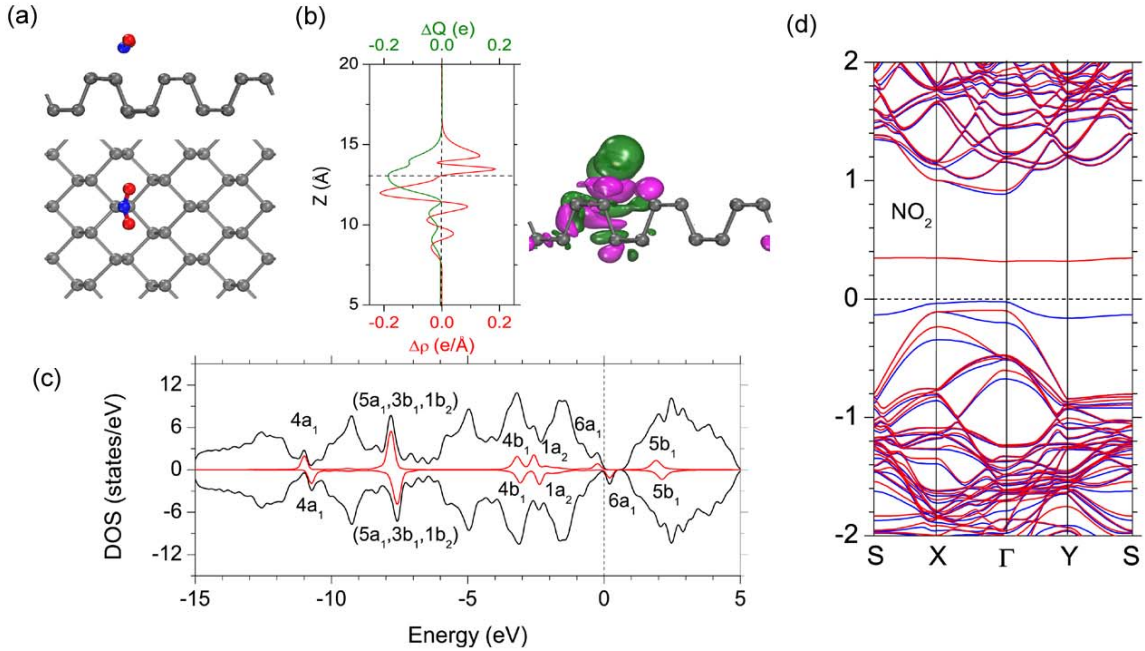


Fig. 6 NO_2 adsorbed on phosphorene. (a) The side and top views of the lowest-energy configuration. The phosphorus, oxygen and nitrogen atoms are represented by balls in grey, red and blue colors, respectively. (b) Plane-averaged differential charge density $\Delta\rho(z)$ (red line), amount of transferred charge $\Delta Q(z)$ (green line), and side view of the 0.005 \AA^{-3} DCD isosurface (right). The violet (green) color denotes diminishing (accumulation) of electrons. (c) DOS of NO_2 on phosphorene (black line) and LDOS and positions of the molecular orbitals of NO_2 (red line). (d) Spin-polarized band structures of NO_2 on phosphorene with spin-up bands and spin-down bands are indicated in blue and red, respectively.

moves above the Fermi level and becomes depopulated after contacting with phosphorene. Therefore, the net gain of electrons from phosphorene results from a strong orbital mixing of HOMO-1 and HOMO-2 states with the 3s states of phosphorus, as reflected by the LDOS analysis as shown in Fig. 5c. This orbital mixing leads to a larger charge transfer induced by the depopulation of the HOMO state, and simultaneously a magnetic moment of $0.63 \mu_B$ of the adsorbed NO. It is noted that the acceptor role of NO on phosphorene is different from that of NO on graphene,¹⁶ in which NO always donates electrons to graphene. It should be noted that a recent work by Kou *et al.*⁴³ predicts a different lowest-energy configuration, with NO binding directly above P atom. This difference could be attributed to the different exchange-correlation functional (LDA) and the vdW corrections (DFT-D2) used in their work. Nevertheless, the oxidation state of NO molecule on phosphorene predicted by both methods is the same. Moreover, our additional calculations show that the “acceptor” character of NO molecule is independent of the anchoring sites on the surface.

NO_2 adsorption: We have placed a single NO_2 molecule on the surface with different orientations: the N-O bonds are oriented up, down or parallel to the surface and aligned along the armchair or zigzag directions. The configuration with the lowest energy is plotted in Fig. 6a. Different from other molecules, the most stable configuration of adsorbed NO_2 is found to be aligned parallel to the zigzag direction with the N atom directly above the P atom and the N-P bond length of 2.27 \AA , which is different from NO_2 adsorption on graphene, where the bonding occurs through both oxygen atoms.²⁰ The NO_2 has the largest binding energy of -0.50 eV among all the studied molecules in present work. It acts as a strong acceptor with a charge transfer from phosphorene to NO_2 of $0.19 e$ based on DCD analysis given in Fig. 6b. It should be noted that our predicted lowest-energy configuration of NO_2 is

different from the recent work⁴³ where the LDA and DFT-D2 were used. Nevertheless, the results of the oxidation state of the bound NO_2 molecule in both works are consistent. According to Fig. 6c and d, the HOMO ($6a_{1,\text{up}}$) is slightly below E_F and the LUMO ($6a_{1,\text{down}}$) is around 0.2 eV above the Fermi energy level E_F . Hence, NO_2 accepts electrons from phosphorene. Similar to NO, charge transfer from phosphorene to NO_2 occurs mainly through orbital hybridization, which simultaneously induces about $0.14 \mu_B$ magnetic moment in phosphorene. This shows that the magnetic properties of phosphorene can be altered through a proper molecular functionalization.

O_2 adsorption: For the oxygen molecule, the most stable configuration is plotted in Fig. 7a, where the O-O bond is aligned along the armchair direction and forms an angle of around 30° with the surface. One of the O atoms is located above the P atom with a O-P bond length of 2.76 \AA , and the binding energy is -0.27 eV . It should be noted that the O_2 molecule adopts a similar adsorption configuration as H_2 with one H or O atom being located right above the P atom, while for CO and NO, the C or N atom is located in the center of the puckered hexagon with a coordination number of four. The underlying reason may be due to the difference in dispersive interactions associated with the non-polar H_2 and O_2 molecules and the polar CO and NO molecules. Similar to NO and NO_2 , O_2 molecule acts as a charge acceptor by gaining about $0.06 e$ from phosphorene, according to Fig. 7b. Clearly, O_2 has a weak physisorption on phosphorene and the O-O bond increases slightly from 1.22 \AA of the free gas molecule to 1.24 \AA for the bound molecule. The orbitals of O_2 is less affected by phosphorene despite a slight broadening of HOMO state ($2\pi, \text{up}$) (Fig. 7c). The antibonding LUMO state ($2\pi, \text{down}$) is nearly unaffected and located in the band gap of phosphorene (Fig. 7d). The magnetic moment of the adsorbed O_2 is around $1.54 \mu_B$, which is slightly quenched from that of the free molecule.

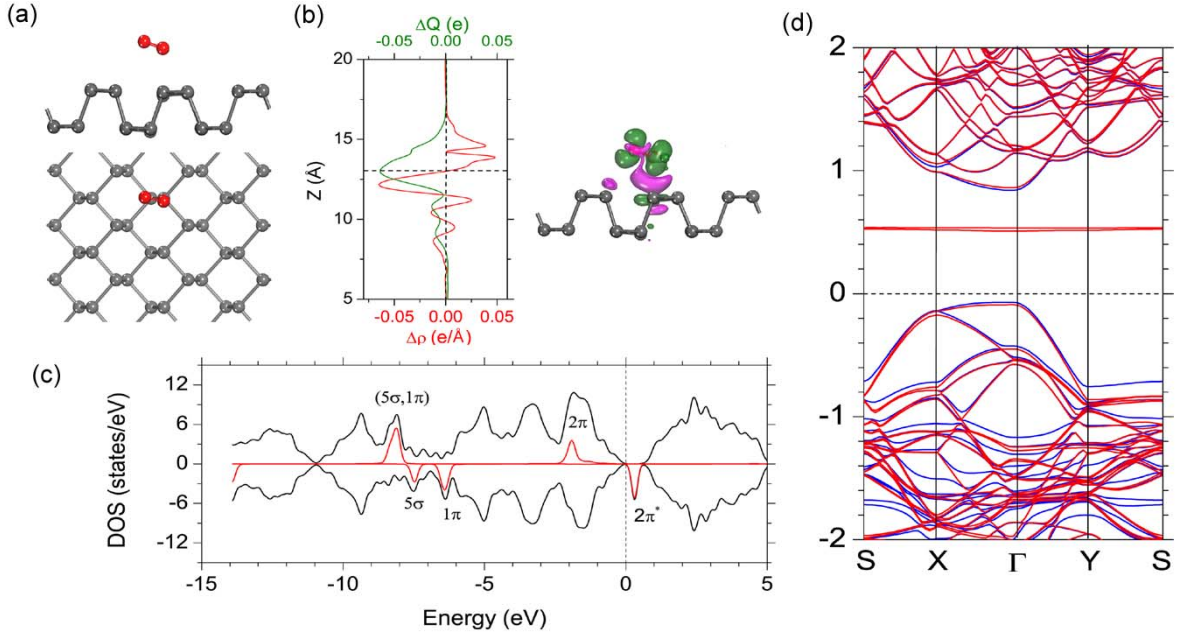


Fig. 7 O₂ adsorbed on phosphorene. (a) The side and top views of the lowest-energy configuration. The phosphorus and oxygen atoms are represented by balls in grey and red colors, respectively. (b) Plane-averaged differential charge density $\Delta\rho(z)$ (red line), amount of transferred charge $\Delta Q(z)$ (green line), and side view of the 0.005 \AA^{-3} DCD isosurface (right). The violet (green) color denotes diminishing (accumulation) of electrons. (c) DOS of O₂ on phosphorene (black line) and LDOS and positions of the molecular orbitals of O₂ (red line). (d) Spin-polarized band structures of O₂ on phosphorene with spin-up bands and spin-down bands are indicated in blue and red, respectively.

Table 1. The binding energy (E_b), the charge transfer (Δq) from molecule to phosphorene, and the X-P bond length (B_{X-P}), where X represents the atom in the molecule. A positive Δq indicates a transfer of electrons from the molecule to phosphorene. We report only the range of lengths where there are several X-P bonds. The oxidation state of the molecule on phosphorene is also listed, and compared with its adsorption on graphene according to Ref. 16.

Molecules	E_b (eV)	Δq (e)	B_{X-P} (Å)	Molecule on Phosphorene	Molecule on Graphene
CO	-0.31	0.007	3.06-3.15	Donor	Donor
H ₂	-0.13	0.013	2.46	Donor	
H ₂ O	-0.14	0.035	2.71	Donor	Acceptor
NH ₃	-0.18	0.050	2.59	Donor	Donor
NO	-0.32	-0.074	2.75-2.88	Acceptor	Donor
NO ₂	-0.50	-0.185	2.27	Acceptor	Acceptor
O ₂	-0.27	-0.064	2.76	Acceptor	

DISCUSSION

Owing to its high mobility, phosphorene is promising for fabricating nanoelectronics devices complementary to graphene. However, phosphorene tends to suffer from the disturbance of chemical interactions from its surrounding molecules. Here, our work shows that phosphorene is electronically polarized upon the physisorption of many small gas molecules. Such a high sensitivity of phosphorene to those physisorbed small molecules renders it promising for gas sensor applications. The marked charge transfer upon exposing phosphorene to H₂O, NH₃, NO, NO₂ and O₂ molecules suggests that molecular physisorption is an effective approach to modulate the carrier density of phosphorene, similar to chemical doping used in a field-effect transistor. Because of its atomically thin thickness, an even moderate charge transfer between phosphorene and the adsorbed molecules can markedly increase its charge carrier density. Previous experiment on MoS₂

has shown that molecular gating can conveniently modulate the carrier density much beyond the dielectric breakdown point.¹⁴

It should be noted that while in the present study, we only considered dilute doping by putting a single molecule on the large supercell. In high doping content, the adsorption energy and the magnitude of charge transfer of each molecule may be different from the prediction here due to the repulsive electrostatic interaction between the adsorbed molecules.³³ We have performed additional calculations by considering two more types of supercell (2×3 and 5×4). Adsorptions of NO and NO₂ are chosen as representatives to identify the lowest-energy configuration among several potential adsorption geometries to consider the size effect. Our results show that the change in supercell size causes a change in absorption configuration for NO molecule, while the absorption configuration for NO₂ molecule seems to be not affected by this change. Since the change in supercell size changes the absorption density, this indicates that the content of the gas can affect the absorption configuration. Interestingly, the oxidation state (“acceptor”) for both molecules is unchanged and thus seems to be independent of the adsorption sites and geometries. Since phos-

phorene displays a large thickness dependence of work function and band gap.³³ future work on the interaction of small molecules physisorbed on multilayer phosphorene is highly desired.

Charge transfer between external molecules and graphene was found to alter the strength of C-C bonds through identifying the shift of Raman G-band.^{54,55} It is expected the charge transfer between external molecules and phosphorene can also alter the strength of P-P bonds. In general, donor molecules are able to strengthen the P-P bonds, whereas acceptor molecules are able to weaken the P-P bonds. Hence, future experimental measurements of the shifts of Raman or IR peaks of the phonon modes is highly desired as the softening or hardening shifts of these frequencies can provide important information for understanding the interaction between external molecules and phosphorene. In addition, we find that all the open-shell molecules (NO, NO₂, and O₂) tend to have a larger binding energy than the closed-shell counterparts, and the adsorbed phosphorenes have new in-gap states induced by the open-shell molecules, which may create new recombination centers for excitons and trigger some new effects on the optical properties of phosphorene.

CONCLUSION

The noncovalent interaction between a number of small molecules and phosphorene is investigated by detailed first-principles calculations. We demonstrate that the physisorbed molecules can significantly alter the electronic properties of phosphorene. NO₂ and NO act as a strong acceptor while NH₃ and H₂O serve as a donor to phosphorene. Owing to the differences in work function between phosphorene and graphene and in the molecular orbital alignment, both NO and H₂O molecules play a distinctively different role in doping phosphorene compared with graphene: NO accepts and H₂O donates electrons upon their adsorption on phosphorene; while NO is a donor and H₂O is an acceptor on graphene. The marked modification in the electronic and magnetic properties of phosphorene induced by the open-shell molecules like NO₂, NO, and O₂, together with a strong binding energy, suggests that phosphorene is promising for molecular sensor applications. The moderate adsorption energy of H₂ may be an advantage for phosphorene to serve as an effective hydrogen storage material at room temperature.

AUTHOR INFORMATION

Corresponding Author

zhangg@ihpc.a-star.edu.sg; zhangyw@ihpc.a-star.edu.sg

Notes

The authors declare no competing financial interests.

ACKNOWLEDGMENT

The authors gratefully acknowledge the financial support from the Agency for Science, Technology and Research (A*STAR), Singapore and the use of computing resources at the A*STAR Computational Resource Centre, Singapore.

REFERENCES

- (1) Dai, J.; Yuan, J. Adsorption of molecular oxygen on doped graphene: Atomic, electronic, and magnetic properties. *Phys. Rev. B* **2010**, *81*, 165414.
- (2) Yu, Y.; Li, C.; Liu, Y.; Su, L.; Zhang, Y.; Cao, L. Controlled scalable synthesis of uniform, high-quality monolayer and few-layer MoS₂ films. *Sci. Rep.* **2013**, *3*, 1866.
- (3) Si, C.; Liu, Z.; Duan, W.; Liu, F. First-principles calculations on the effect of doping and biaxial tensile strain on

- electron-phonon coupling in graphene. *Phys. Rev. Lett.* **2013**, *111*, 196802.
- (4) Chen, X.; Liu, Y.; Gu, B.-L.; Duan, W.; Liu, F. Giant room-temperature spin caloritronics in spin-semiconducting graphene nanoribbons. *Phys. Rev. B* **2014**, *90*, 121403.
- (5) Ke, Q.; Tang, C.; Liu, Y.; Liu, H.; Wang, J. Intercalating graphene with clusters of Fe₃O₄ nanocrystals for electrochemical supercapacitors. *Mater. Res. Express* **2014**, *1*, 025015.
- (6) Ke, Q.; Liu, Y.; Liu, H.; Zhang, Y.; Hu, Y.; Wang, J. Surfactant-modified chemically reduced graphene oxide for electro-chemical supercapacitors. *RSC Advance* **2014**, *4*, 26398-26406.
- (7) Cai, Y.; Zhang, G.; Zhang, Y.-W. Polarity-reversed robust carrier mobility in monolayer MoS₂ nanoribbons. *J. Am. Chem. Soc.* **2014**, *136*, 6269-6275.
- (8) Cai, Y.; Lan, J.; Zhang, G.; Zhang, Y.-W. Lattice vibrational modes and phonon thermal conductivity of monolayer MoS₂. *Phys. Rev. B* **2014**, *89*, 035438.
- (9) Liu, X.; Zhang, G.; Pei, Q.-X.; Zhang, Y.-W. Phonon thermal conductivity of monolayer MoS₂ sheet and nanoribbons. *Appl. Phys. Lett.* **2013**, *103*, 133113.
- (10) Yin, Z.; Zhang, X.; Cai, Y.; Chen, J.; Wong, J. I.; Tay, Y.-Y.; Chai, J.; Wu, J.; Zeng, Z.; Zheng, B.; Yang, H. Y.; Zhang, H. Preparation of MoS₂-MoO₃ hybrid nanomaterials for light-emitting diodes. *Angew. Chem.* **2014**, *126*, 1-7.
- (11) Li, H.; Wu, J.; Yin, Z. Y.; Zhang, H. Preparation and applications of mechanically exfoliated single- and multi-layer MoS₂ and WSe₂ nanosheets. *Acc. Chem. Res.* **2014**, *47*, 1067-1075.
- (12) He, Q. Y.; Zeng, Z. Y.; Yin, Z. Y.; Li, H.; Wu, S. X.; Huang, X.; Zhang, H. Fabrication of flexible MoS₂ thin-film transistor arrays for practical gas-sensing applications. *Small* **2012**, *8*, 2994-2999.
- (13) Liu, B.; Chen, L.; Liu, G.; Abbas, A. N.; Fathi, M.; Zhou, C. High-performance chemical sensing using schottky-contacted chemical vapor deposition grown monolayer MoS₂ transistors. *ACS Nano* **2014**, *8*, 5304-5314.
- (14) Mehmood, F.; Pachter, R. Density functional theory study of chemical sensing on surfaces of single-layer MoS₂ and graphene. *J. Appl. Phys.* **2014**, *115*, 164302.
- (15) Crowther, A. C.; Ghassaei, A.; Jung, N.; Brus, L. E. Strong charge-transfer doping of 1 to 10 layer graphene by NO₂. *ACS Nano* **2012**, *6*, 1865-1875.
- (16) Leenaerts, O.; Partoens, B.; Peeters, F. M. Adsorption of H₂O, NH₃, CO, NO₂, and NO on graphene: A first-principles study. *Phys. Rev. B* **2008**, *77*, 125416.
- (17) Chen, L.; Wang, L.; Shuai, Z.; Beljonne, D. Energy level alignment and charge carrier mobility in noncovalently functionalized graphene. *J. Phys. Chem. Lett.* **2013**, *4*, 2158-2165.
- (18) Elias, D. C.; Nair, R. R.; Mohiuddin, T. M. G.; Morozov, S. V.; Blake, P.; Halsall, M. P.; Ferrari, A. C.; Boukhvalov, D. W.; Katsnelson, M. I.; Geim, A. K.; Novoselov, K. S. Control of graphene's properties by reversible hydrogenation: Evidence for graphane. *Science* **2009**, *323*, 610.
- (19) Cai, Y.; Bai, Z.; Pan, H.; Feng, Y. P.; Yakobson, B. I.; Zhang, Y.-W. Constructing metallic nanoroad on MoS₂ monolayer via hydrogenation. *Nanoscale* **2014**, *6*, 1691-1697.
- (20) Zhou, M.; Lu, Y.-H.; Cai, Y.-Q.; Zhang, C.; Feng, Y.-P. Adsorption of gas molecules on transition metal embedded graphene: A search for high performance graphene-based catalysts and gas sensors. *Nanotechnology* **2011**, *22*, 385502.
- (21) Xiao, J.; Long, M.; Li, X.; Zhang, Q.; Xu, H.; Chan, K. S. Effects of van der Waals interaction and electric field on the electronic structure of bilayer MoS₂. *J. Phys.: Condens. Matter* **2014**, *26*, 405302.
- (22) Chen, Z.; Darancet, P.; Wang, L.; Crowther, A. C.; Gao, Y.; Dean, C. R.; Taniguchi, T.; Watanabe, K.; Hone, J.; Marianetti, C. A.; Brus, L. E. Physical adsorption and charge transfer of molecular Br₂ on graphene. *ACS Nano* **2014**, *8*, 2943-2950.

- (23) Singh, K.; Uddin, M. A.; Tolson, J. T.; Maire-Afeli, H.; Sbrockey, N.; Tompa, G. S.; Spencer, M. G.; Vogt, T.; Sudarshan, T. S.; Koley, G. Electrically tunable molecular doping of graphene. *Appl. Phys. Lett.* **2013**, *102*, 043101.
- (24) Late, D. J.; Huang, Y.-K.; Liu, B.; Acharya, J.; Shirodkar, S. N.; Luo, J.; Yan, A.; Charles, D.; Waghmare, U. V.; Dravid, V. P.; Rao, C. N. R. Sensing behavior of atomically thin-layered MoS₂ transistors. *ACS Nano* **2013**, *7*, 4879–4891.
- (25) Li, H.; Yin, Z. Y.; He, Q. Y.; Li, H.; Huang, X.; Lu, G.; Fam, D. W. H.; Tok, A. I. Y.; Zhang, Q.; Zhang, H. Fabrication of single- and multilayer MoS₂ film-based field-effect transistors for sensing NO at room temperature. *Small* **2012**, *8*, 63–67.
- (26) Huang, B.; Li, Z.; Liu, Z.; Zhou, G.; Hao, S.; Wu, J.; Gu, B.-L.; Duan, W. Adsorption of gas molecules on graphene nanoribbons and its implication for nanoscale molecule sensor. *J. Phys. Chem. C* **2008**, *112*, 13442–13446.
- (27) Hu, T.; Gerber, I. C. Theoretical study of the interaction of electron donor and acceptor molecules with graphene. *J. Phys. Chem. C* **2013**, *117*, 2411–2420.
- (28) Liu, H.; Neal, A. T.; Zhu, Z.; Luo, Z.; Xu, X.; Tománek, D.; Ye, P. D. Phosphorene: an unexplored 2D semiconductor with a high hole mobility. *ACS Nano* **2014**, *8*, 4033–4041.
- (29) Brown, A.; Rundqvist, S. Refinement of the crystal structure of black phosphorus. *Acta Cryst.* **1965**, *19*, 684.
- (30) Li, L.; Yu, Y.; Ye, G. J.; Ge, Q.; Ou, X.; Wu, H.; Feng, D.; Chen, X. H.; Zhang, Y. Black phosphorus field-effect transistors. *Nature Nanotech.* **2014**, *9*, 372.
- (31) Zhao, S.; Kang, W.; Xue, J. The potential application of phosphorene as an anode material in Li-ion batteries. *J. Mater. Chem. A* **2014**, *2*, 19046–19052.
- (32) Guan, J.; Zhu, Z.; Tománek, D. Phase coexistence and metal-insulator transition in few-layer phosphorene: A computational study. *Phys. Rev. Lett.* **2014**, *113*, 046804.
- (33) Cai, Y.; Zhang, G.; Zhang, Y.-W. Layer-dependent band alignment and work function of few-layer phosphorene. *Scientific Reports*, **2014**, 6677.
- (34) J. Dai and X. C. Zeng, Bilayer phosphorene, effect of stacking order on bandgap and its potential applications in thin-film solar cells. *J. Phys. Chem. Lett.* **2014**, *5*, 1289–1293.
- (35) Li, W.; Zhang, G.; Zhang, Y.-W. Electronic properties of edge-hydrogenated phosphorene nanoribbons: A first-principles study. *J. Phys. Chem. C* **2014**, *118*, 22368–22372.
- (36) Wang, L.; Sofer, Z.; Pumbera, M. Voltammetry of layered black phosphorus: Electrochemistry of multilayer phosphorene. *Chemelectrochem*. DOI: 10.1002/celec.201402363.
- (37) Peng, X.; Wei, Q.; Copple, A. Strain-engineered direct-indirect band gap transition and its mechanism in two-dimensional phosphorene. *Phys. Rev. B* **2014**, *90*, 085402.
- (38) Qiao, J.; Kong, X.; Hu, Z.-X.; Yang, F.; Ji, W. High-mobility transport anisotropy and linear dichroism in few-layer black phosphorus. *Nat. Comm.* **2014**, *5*, 4475.
- (39) Xia, F.; Wang, H.; Jia, Y. Rediscovering black phosphorus as an anisotropic layered material for optoelectronics and electronics. *Nat. Comm.* **2014**, *5*, 4458.
- (40) Tran, V.; Soklaski, R.; Liang, Y.; Yang, L. Layer-controlled band gap and anisotropic excitons in few-layer black phosphorus. *Phys. Rev. B* **2014**, *89*, 235319.
- (41) Kresse, G.; Furthmüller, J. Efficient iterative schemes for ab initio total-energy calculations using a plane-wave basis set. *Phys. Rev. B* **1996**, *54*, 11169.
- (42) Becke, A. D. Density-functional exchange-energy approximation with correct asymptotic behavior. *Phys. Rev. A* **1988**, *38*, 3098.
- (43) Kou, L.; Frauenheim, T.; Chen, C. Phosphorene as a superior gas sensor: Selective adsorption and distinct IV response. *J. Phys. Chem. Lett.* **2014**, *5*, 2675–2681.
- (44) Ding, F.; Yakobson, B. I. Challenges in hydrogen adsorptions: From physisorption to chemisorptions. *Front. Phys.* **2011**, *6*, 142–150.
- (45) Fair, K. M.; Cui, X. Y.; Li, L.; Shieh, C. C.; Zheng, R. K.; Liu, Z. W.; Delley, B.; Ford, M. J.; Ringer, S. P.; Stampfl, C. Hydrogen adsorption capacity of adatoms on double carbon vacancies of graphene: A trend study from first principles. *Phys. Rev. B* **2013**, *87*, 014102.
- (46) Wang, S. C.; Senbetu, L.; Woo, C. Superlattice of parahydrogen physisorbed on graphite surface. *J. Low Temp. Phys.* **1980**, *41*, 611.
- (47) Goler, S.; Coletti, C.; Tozzini, V.; Piazza, V.; Mashoff, T.; Beltram, F.; Pellegrini, V.; Heun, S. Influence of graphene curvature on hydrogen adsorption: Toward hydrogen storage devices. *J. Phys. Chem. C* **2013**, *117*, 11506–11513.
- (48) Tozzini, V.; Pellegrini, V. Reversible hydrogen storage by controlled buckling of graphene layers. *J. Phys. Chem. C* **2011**, *115*, 25523–25528.
- (49) Cheng, H.; Cooper, A. C.; Pez, G. P.; Kostov, M. K.; Pitrowski, P.; Stuart, S. J. Molecular dynamics simulations on the effects of diameter and chirality on hydrogen adsorption in single walled carbon nanotubes. *J. Phys. Chem. B* **2005**, *109*, 3780–3786.
- (50) Park, S.; Srivastava, D.; Cho, K. Generalized chemical reactivity of curved surfaces: Carbon nanotubes. *Nano Lett.* **2003**, *3*, 1273–1277.
- (51) Boukhvalov, D. W.; Katsnelson, M. I. Enhancement of chemical activity in corrugated graphene. *J. Phys. Chem. C* **2009**, *113*, 14176–14178.
- (52) González, B. S.; Hernández-Rojas, J.; Bretón, J.; Gomez Llorente, J. M. Global potential energy minima of (H₂O)_n clusters on graphite. *J. Phys. Chem. C* **2007**, *111*, 14862.
- (53) Cai, Y.; Bai, Z.; Chintalapati, S.; Zeng, Q.; Feng, Y. P. Transition metal atoms pathways on rutile TiO₂ (110) surface: Distribution of Ti³⁺ states and evidence of enhanced peripheral charge accumulation. *J. Chem. Phys.* **2013**, *138*, 154711.
- (54) Das, B.; Voggu, R.; Rout, C. S.; Rao, C. N. R. Changes in the electronic structure and properties of graphene induced by molecular charge-transfer. *Chem. Commun.* **2008**, 5155.
- (55) Choudhury, D.; Das, B.; Sarma, D. D.; Rao, C. N. R. XPS evidence for molecular charge-transfer doping of graphene. *Chem. Phys. Lett.* **2010**, *497*, 66–69.

